

# Morphology and Crystallization Kinetics of it-Polystyrene Spherulites

Hiroshi Kajioka, Shigeru Yoshimoto, Ken Taguchi, and Akihiko Toda\*

Graduate School of Integrated Arts and Sciences, Hiroshima University, Higashi-Hiroshima 739-8521, Japan

Received December 27, 2009; Revised Manuscript Received March 17, 2010

**ABSTRACT:** Based on our recent proposal for the formation mechanism of polymer spherulites, the correlation between the morphology and crystallization kinetics has been examined for it-polystyrene (itPS) spherulites grown from the melt down to temperatures near the glass transition,  $T_g$ . The inner structure of the nonbanded spherulites of itPS has been characterized by the persistence length of the patchy pattern observed by polarizing optical microscopy. The persistence length was in proportion to the width of lamellar crystals at the growth front, which was observed by atomic force microscopy. The result reconfirms our suggestion that the inner structure of spherulites is determined by the size of the building blocks. For the determination mechanism of the width of lamellae, the possibility of instability-driven branching has been examined by the correlation between the characteristic lengths and the growth rate in terms of the temperature dependence near  $T_g$ . The correlation followed the dependence predicted for the two cases of the instability caused by the compositional gradient and by the pressure gradient. The compositional gradient is determined by the self-diffusion of polymer chains and the pressure gradient by the melt viscosity. Near  $T_g$ , owing to the development of spatial heterogeneity, the decoupling of self-diffusion from the melt viscosity can be expected. By examining the possible decoupling, the cases were dismissed for the influence of self-diffusion of portions of polymer chain on crystallization at the growth front and for the compositional gradient formed by small uncrystallized molecules.

## 1. Introduction

Spherulite is the basic higher order structure of crystalline polymers. The structure is composed of lamellar crystals filling in the inner part by the repetition of reorientation and branching on the growth in the radial direction. In our recent studies<sup>1–4</sup> aiming to clarify the formation mechanism, we have examined the correlation among the growth rate, the size of lamellar crystallites at the growth front, and the characteristic length of the inner structure of spherulites. The examined results of the spherulites of polyethylene (PE),<sup>1,4</sup> poly(vinylidene fluoride) (PVDF),<sup>2</sup> and isotactic poly(butene-1) (itPBI)<sup>3</sup> suggested the followings.

(1) The inner structure of spherulites is basically determined by the width of the building blocks, that is, the width of lamellar crystals at the growth front. This relationship simply means that coarser inner structure is formed by wider lamellae, and vice versa. The inner structure is represented by the pattern seen under polarizing optical microscopy, such as the concentric bands in banded spherulites and the patchy pattern in nonbanded spherulites, as shown in Figure 1. The concentric rings are the consequences of successive lamellar twisting along the radial direction, which is coherent along the tangential direction. The patchy pattern in nonbanded spherulites, on the other hand, suggests the loss of coherence or a random reorientation of lamellar crystals on growth. The patterns are therefore determined by the correlation of lamellar orientation along the radial direction in those spherulites, so that the proportional relationship between the characteristic size of inner structure and the width of lamellae suggests the mechanism of lamellar reorientation which must be easier for narrower lamellae.

(2) The width of lamellar crystals is determined by the dynamical coupling of the reorientation due to an intrinsic strain and the branching which is driven by an instability. In terms of the

intrinsic strain, as has been discussed by Lotz and Cheng<sup>5</sup> in detail, the molecular structure of chain foldings will be the origin of the intrinsic and unbalanced surface stresses. On the other hand, for the instability, we have supposed a gradient field spontaneously formed in the melt in the vicinity of the growth front. The origin of the gradient field can be compositional as has been proposed by Keith and Padden,<sup>6</sup> which is formed by uncrystallized materials rejected at the growth front. The gradient field can also be created by the density difference between the crystal and the melt, as has been supposed by Schultz.<sup>7</sup> Usually, crystal density is higher than that of the melt, so that there must be a flow to supply crystallizing materials to the growth front in order to continue the stationary growth. Then, the flow should be driven by a pressure gradient in the melt, namely, there must be a negative pressure at the growth front. In both cases of the compositional gradient and the pressure gradient, the gradient introduces the gradient in free energy near the growth front in the melt; the closer to the growth front, the lower the free energy of the melt.

In the gradient field, when a growth front sticks out from the mean position into the melt by fluctuation, the part feels larger driving force and the fluctuation is accelerated. The surface tension of crystals meanwhile suppresses the fluctuation having large curvature, and hence the balance between those two effects determines the condition for the growth of small branches by fluctuation and the resultant critical width of growth front. The lamellar crystals reaching the critical width undergo the instability to be split into small branches. The small branches will then be reoriented due to the intrinsic strain, and start to grow independently from each other in the three-dimensional space. The independent growth means not only the growth in the radial direction of spherulite but also the growth in width, so that the width reaches the critical value again. By this mechanism, the branching and reorientation will be repeated at the growth front to fill in the space with lamellar branches to form well developed polymer spherulite.

\*Corresponding author: tel +81-82-424-6558, fax +81-82-424-0757, e-mail atoda@hiroshima-u.ac.jp.

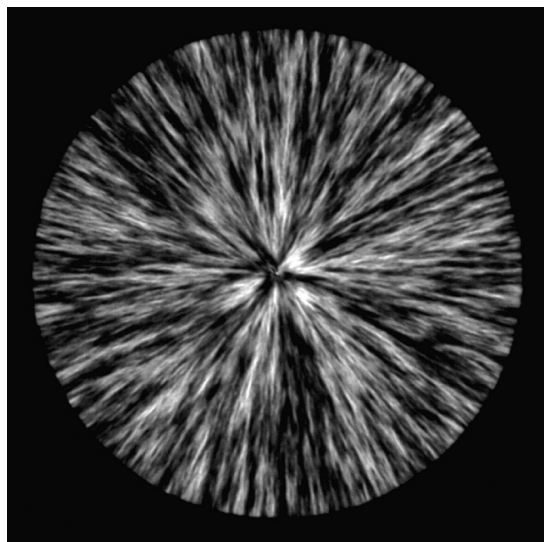


**Figure 1.** POM image of a nonbanded spherulite of isotactic polystyrene. The image was obtained by the sum of two images of the same area differing in the angle of polarizer by  $45^\circ$  while keeping the condition of cross-nicols. The image size is  $200\ \mu\text{m} \times 200\ \mu\text{m}$ .

For the two cases of possible gradient fields, the following equations represent the relationship among the growth rate,  $V$ , the size of lamellar crystallites at the growth front,  $\lambda$ , and the characteristic length of the inner structure of spherulites,  $L$ ,

$$L \propto \lambda \propto (\gamma D/V)^{1/2} \quad \text{compositional} \quad (1)$$

$$\propto (\gamma/\eta V)^{1/2} \quad \text{pressure} \quad (2)$$

where  $\gamma$  represents the surface tension,  $D$  the diffusion coefficient for compositional gradient, and  $\eta$  the viscosity for pressure gradient. In the expression of eqs 1 and 2,  $D$  and  $1/\eta$  are believed to change almost in the same way owing to the Einstein relationship between them, i.e.,  $D \propto k_B T/\eta$ . Therefore, for a given material examined, both equations predict almost the same dependences on the applied conditions, so that the experimental distinction between them for the identical material is in principle not possible. Actually, the examination in terms of the temperature dependence has successfully confirmed the relationships represented by eq 1 or 2 for the spherulites of PE,<sup>1,4</sup> PVDF,<sup>2</sup> and iPB1<sup>3</sup> but did not identify the physical origin of the gradient, whether it is compositional or pressure gradient.

In order to make the distinction, we need to utilize the characteristics of different materials of the same kind, e.g., the molar mass. We know that the molar mass dependences of the diffusion coefficient and the viscosity are different as follows:  $D \propto M_w^{-2}$  and  $\eta^{-1} \propto M_w^{-3.4 \sim -3.6}$ .<sup>8</sup> By examining the molar mass dependence for polyethylene having different average molar mass, we have obtained the following results

$$L^2 V \propto M_w^{-3.5} \quad \text{and} \quad \lambda^2 V \propto M_w^{-3.7} \quad (3)$$

which have clearly suggested that the viscosity is related to the physical mechanism, so that it has been concluded that the pressure gradient is responsible for the instability, at least, in the case of polyethylene.<sup>4</sup>

In the present paper, we examine another approach to do the distinction. As discussed in the above, under ordinary equilibrium conditions, owing to the Einstein's relationship, the diffusion coefficient and the inverse of viscosity behave almost in the same way. However, under the conditions near the glass transition temperature, the development of spatial heterogeneity in the melt brings some anomalous behaviors in the dynamics.

Isotactic polystyrene (iPS) is a well-known polymer to be crystallized isothermally over a wide temperature range down to near the glass transition temperature,  $T_g$ . In terms of the temperature dependence of iPS crystallization, the following unusual behavior is known to occur near  $T_g$ . In the standard model of polymer crystallization, i.e., Lauritzen–Hoffman model,<sup>9</sup> polymer crystallization is believed to be determined by two basic factors, i.e., surface nucleation barrier and the mobility of crystallizing molecules. Among them, the mobility factor is usually believed to be inversely proportional to viscosity, but for iPS the temperature dependence of crystal growth rate near  $T_g$  cannot be properly adjusted by that of viscosity.<sup>9</sup> Considering the fact that the motion of crystallizing polymer chain involves a length significantly smaller than its total contour length, the deviation has been ascribed to a specific mobility of the crystallizing portion at the growth front, the mobility of which can be different from that of the whole molecule in the bulk melt.<sup>9</sup>

In terms of the possible decoupling of mobility factor from viscosity in the bulk melt near  $T_g$ , it is known that the explicit form of Einstein's relationship, i.e., the Stokes–Einstein relation of  $D_s = k_B T/(6\pi\eta r)$ , is broken down for the melt composed of molecules of radius,  $r$ , under the conditions of  $T < 1.2T_g$ .<sup>10</sup> The breakdown is due to the fact that the diffusion coefficient and the viscosity see different characteristics of the dynamical properties of the melt. It means that the diffusion coefficient is determined by the fastest pass for diffusion, while the viscosity sees the dynamics averaged over surrounding environment and is influenced by slower regions. As far as the system is in equilibrium and homogeneous, the diffusion is coupled with the viscosity. Near  $T_g$ , on the other hand, because of the development of spatial heterogeneity in the melt, the characteristic of diffusion decouples from that of viscosity to have diffusion faster than that predicted from the Stokes–Einstein relation:  $D_s > k_B T/(6\pi\eta r)$  by 3 or 4 orders in magnitude at  $T_g$ , depending on the size of the molecules;<sup>11,12</sup> smaller molecules have larger deviation. Based on the anomaly, even though the decoupling is known to be limited only to small molecules, the motions of portion of long-chain molecule in the crystallization process can have the characteristic jump rate different from that of viscosity of the whole molecule in the bulk melt.<sup>9</sup> Here, it needs to be mentioned that our proposal of the structural evolution due to a gradient field is believed to be determined by the global viscosity or self-diffusion of a whole molecule in the bulk melt. We will be able to examine the influence of the mobility of crystallizing chains on the correlation between the kinetics and morphology. Another possible examination near  $T_g$  by utilizing the decoupling will be the distinction of the mobility of small molecules as an impurity for crystallization. If small molecules behave as an impurity, the molecules will build up concentration gradient near the growth front, which can be a candidate for the origin of the structural evolution of the instability. If it is the case, we can distinguish the compositional gradient formed by small molecules by examining the temperature dependence, which will decouple from that with viscosity near  $T_g$ .

Concerned with the inner structure of spherulites, iPS is known to form inherently nonbanded spherulites without concentric banding under any crystallization conditions. For the inherently nonbanded spherulites, the reorientation of lamellar crystals is believed to occur in random directions on growth. We have recently proposed to characterize the inner structure by the correlation length of the patchy pattern seen in this type of spherulites by polarizing optical microscopy (POM)<sup>3</sup> (Figure 1). On the other hand, in terms of the microstructural evolution in iPS spherulites, the lamellar morphology have been studied in

detail by Keith and Padden<sup>13,14</sup> and Bassett and Vaughan,<sup>15,16</sup> but the examination has been focused on the morphology far above  $T_g$  in those studies.

On the basis of those preceding studies on the kinetics and morphology of polymer crystallization, in the present report, we examine the crystallization of itPS near  $T_g$  in terms of the growth rate, the characteristic length of the nonbanded spherulites by utilizing POM, and the width of lamellar crystals at the growth front, which are observed by atomic force microscopy (AFM) for the samples isothermally crystallized, quenched, and then chemically etched.

## 2. Experimental Section

Isotactic poly(styrene) ( $M_w = 556\,000$ ,  $M_w/M_n = 1.9$ ) was purchased from Polymer Laboratories Ltd.; the nominal melting region was 205–225 °C. The polymer forms nonbanded and large spherulites ( $\sim 300\ \mu\text{m}$ ). Thin films of ca.  $1\ \mu\text{m}$  thick were prepared by spin-coating from cyclohexanone solution. Films thicker than  $3\ \mu\text{m}$  were prepared by pressing the powder on a hot plate between cover glasses or between a cover glass and an aluminum foil. The films were quenched to room temperature after the preparation, so that they were basically in the amorphous state.

For crystallization, the film was first kept at 240–280 °C for 2 min to erase thermal history. The film was then crystallized isothermally at 120–210 °C and quenched to stop the growth. Because of slow crystallization of itPS ( $< 20\ \mu\text{m/h}$ ), the influence of crystallization during those temperature jumps was negligible. In order to avoid degradation of itPS, the thermal treatments were done with the films covered by a pair of glasses or a glass and an aluminum foil or done under vacuum for free surfaces. It has also been checked that the crystallization in air can be conducted without the influence of degradation on the kinetics and morphology if the set time at temperatures below 200 °C was short enough less than ca. 1 h.

For the microscopic examination of lamellar crystals at the growth front of spherulites, the surrounding amorphous portions were removed by permanganic etching under the same condition as utilized by Vaughan and Bassett<sup>16</sup> for itPS. The samples were then examined with an atomic force microscope, AFM (SPI3800N, Seiko Instruments Inc.), in a dynamic force mode in air at room temperature. Silicon cantilevers (SI-DF20, Seiko Instruments Inc.) with a resonance frequency of 110–150 kHz were used for the observations. By AFM, we have measured the lateral width of crystals at the growth front. We have determined the maximum lamellar width,  $\lambda$ , by averaging the size of several large crystals, which were placed at the growth front of different locations in spherulites. The data scatter was as much as  $\pm 40\%$ .

With a polarizing optical microscope, POM (BX51, Olympus Corp.), itPS spherulites were examined for the measurements of the inner structure and the growth rate from the change in size with crystallization time. The POM image shown in Figure 1 is the sum of two images of the same area differing in the angle of polarizer by 45° while keeping the condition of cross-nicols. This pattern of nonbanded spherulites without the Maltese cross is characterized by the patchy pattern representing the orientation correlation of crystalline fibrils along the radial direction. For this type of image, we have defined an autocorrelation function in terms of the square root of the POM intensity,  $I(x)^{0.5}$ , as a function of the distance,  $d$ , along the radial ( $x$ ) direction, as follows:

$$C(d) \equiv \frac{\langle I(x+d, y)^{0.5} I(x, y)^{0.5} \rangle - \langle I(x, y)^{0.5} \rangle^2}{\langle I(x, y) \rangle - \langle I(x, y)^{0.5} \rangle^2} \quad (4)$$

where  $y$  represents the coordinate perpendicular to  $x$  and the angle brackets  $\langle \rangle$  represent the statistical average for the two-dimensional map.<sup>3</sup> The correlation function was fit by the following approximate form showing an exponential decay

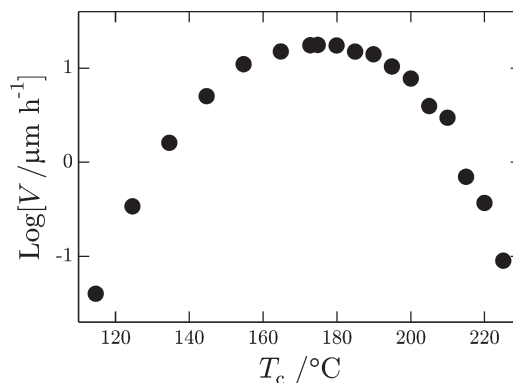


**Figure 2.** Linear growth rate,  $V$ , of itPS plotted against crystallization temperature.

with the persistence length,  $L$ , of the pattern along the radial direction

$$C(d) \sim \exp\left[-\frac{d}{L}\right] + \frac{d}{L} \exp\left[-\frac{d}{\alpha}\right] \quad (5)$$

where the parameter  $\alpha$  represents the effects of the optical resolution limit and the basic length of crystalline fibrils and is much shorter than  $L$ ; the details of the approximate form will be discussed elsewhere.<sup>17</sup> In some cases, a monochromatic filter (IF550, Olympus Co Ltd.) was used, but the filtering was not essential in the determination procedure.

## 3. Results and Discussion

Figure 2 shows the temperature dependence of growth rate,  $V$ . As is well-known, the growth rate of polymer crystals shows a bell-shaped dependence limited by the melting temperature,  $T_m$ , and  $T_g$ . In the standard model of polymer crystallization by Lauritzen and Hoffman,<sup>9</sup> the growth is controlled by the formation of surface nucleation on the growth face, and the growth velocity,  $V$ , is represented as

$$V = V_0 \exp\left[-\frac{K}{fT\Delta T}\right] \quad (6)$$

where  $V_0$  represents the frequency factor determined by the mobility of molecules, and the exponential term represents the surface nucleation barrier with the applied supercooling,  $\Delta T \equiv T_m - T$ , and a constant,  $K$ , determined by the surface free energies, the heat of fusion, and  $T_m$ . Here, the additional coefficient,  $f$ , is for the correction of the driving force at larger supercoolings:  $f = 2T/(T + T_m)$ . In the standard procedure of the analysis, the frequency factor,  $V_0$ , is assumed to be in proportion to the inverse of viscosity, i.e.,  $V_0 \propto \eta^{-1}$ . The temperature dependence of viscosity,  $\eta_T \equiv \eta(T)/\eta(T_g)$ , is expressed by that of Vogel–Fulcher type and is well-known as the WLF equation<sup>18</sup> represented as follows:

$$\log \eta_T = -\frac{c_1(T - T_g)}{c_2 + T - T_g} \quad (7)$$

where the constants are set at  $c_1 = 17.44$  and  $c_2 = 51.6\ \text{K}$  as “universal” constants. For PS, the experimentally determined coefficients are available from literatures<sup>19</sup> as  $c_1 = 17.4$  and  $c_2 = 52.1\ \text{K}$ , which are close to the “universal” constants.

In this way, eq 6 predicts that the growth rate multiplied by the temperature dependence of viscosity,  $V\eta_T$ , will be on a straight line in the semilogarithmic plot against  $1/fT\Delta T$ . However, as is recognized in the semilogarithmic plots in Figure 3, it is



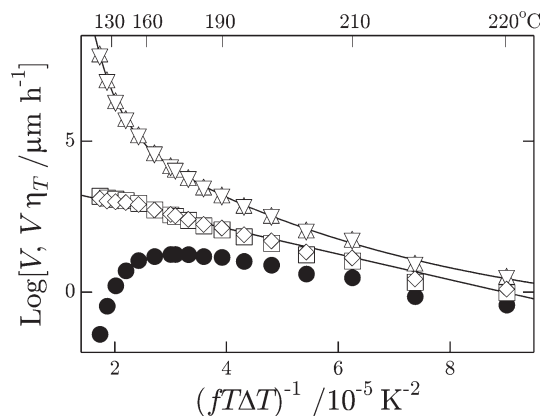


**Figure 3.** Semilogarithmic plots against  $(fT\Delta T)^{-1}$  of  $V$  (●),  $V\eta_T$  (WLF, △; EXP, ▽), and  $V\eta_T'$  (HOF, □; EXP, ◇).

well-known that the plot of  $V\eta_T$  for the growth rate data of itPS near  $T_g$  cannot be fitted by a single straight line in the plot against  $1/fT\Delta T$ , where the literature values of  $T_m = 242\text{ °C}$ <sup>9</sup> and  $T_g = 99.8\text{ °C}$ <sup>19</sup> were employed. Hoffman<sup>9</sup> has supposed that the deviation is due to the specific mobility of crystallizing portion of polymer chain at the growth front; the mobility can be different from that in the bulk melt. Then, Hoffman proposed to adjust the parameters,  $c_1$  and  $c_2$ , of eq 7 to get a straight line in the plot of  $V\eta_T'$ . Here, the temperature dependence of  $\eta_T'$  is expressed as eq 7 with adjusted values of the coefficients for the best fit by a straight line in the semilogarithmic plot of  $V\eta_T'$  against  $1/fT\Delta T$ . For itPS, the coefficients determined by Hoffman were  $c_1' = 11.4$  and  $c_2' = 30\text{ K}$ : i.e.,  $\eta_T' = \exp[1560/R(T - T_g + 30)]$  with the gas constant,  $R = 1.986\text{ cal/K mol}$ . With those coefficients chosen, the temperature dependence of  $\eta_T'$  becomes much milder than that of bulk viscosity,  $\eta_T$ , near  $T_g$ . It is known that the nonstandard values of the constants,  $c_1'$  and  $c_2'$ , are believed to apply to the crystallization kinetics of all polymers reported so far. However, the influence becomes significant for the crystallization near  $T_g$ , which can be realized with itPS. It is also noted that poly(*p*-phenylene sulfide) can also be crystallized in a wide temperature range down to near  $T_g$ , and even with the nonstandard values of the constants,  $V\eta_T'$  showed an inflection, which has been successfully explained as the regime II–III transition with the slope ratio close to two.<sup>20</sup> In Figure 3,  $V\eta_T$  (WLF) represents the results with WLF's "universal" constants,<sup>18</sup>  $V\eta_T$  (EXP) with the experimentally determined coefficients,<sup>19</sup>  $V\eta_T'$  (HOF) with Hoffman's constants, and  $V\eta_T'$  (EXP) with the coefficients,  $c_1' = 8.3$  and  $c_2' = 33\text{ K}$ , for the best fit of the present experimental data to get a straight line.

The results shown in Figure 3 suggest that the temperature dependence of  $\eta_T'$  is much smaller than that of  $\eta_T$  near  $T_g$  and imply faster mobility for crystallization near  $T_g$  in comparison with that of  $\eta_T$ . This deviation is in the same direction as the decoupling of diffusion from the Einstein's relation, though the possibility of decoupling has been dismissed for the self-diffusion of whole polymer chain,<sup>12</sup> with which the spatial heterogeneity is believed to be averaged. We think that there can still be a possibility of decoupling of the mobility for the part of polymer chains crystallizing at the growth front; the effective mobility for crystallization will be that of a portion of polymer chain, so that the mobility can be without the averaging the surrounding environment and is different from that in the bulk melt. By utilizing the temperature dependence of growth rate,  $V$ , multiplied by  $\eta_T$  obtained from the literature and by  $\eta_T'$  determined by the adjustment of the parameters, it is possible to examine the temperature dependences of the morphological changes in the persistence length,  $L$ , and in the lamellar width at the growth front,  $\lambda$ , in the plots against  $V\eta_T$  and  $V\eta_T'$ , as expected from eq 2

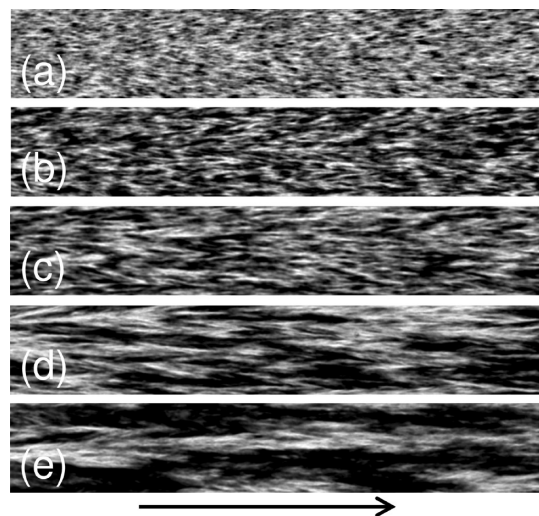


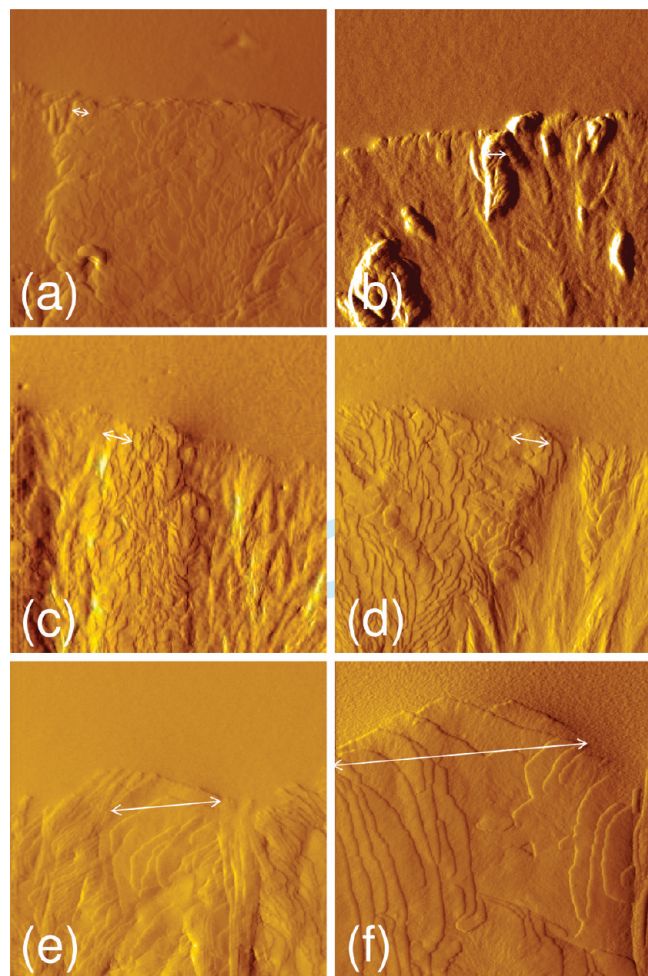
**Figure 4.** POM images of the portions of itPS spherulites. Crystallization temperatures were (a) 150, (b) 160, (c) 170, (d) 180, and (e) 190 °C. The images were processed as in Figure 1. The radial direction of spherulites is indicated by the arrow. The image size is  $300\text{ }\mu\text{m} \times 50\text{ }\mu\text{m}$ .

to see either of the mobility coefficients is effective for the structural evolution. The possibility of compositional gradient formed by small molecules can also be checked by those dependences in comparison with those expected from eq 1, for which the breakdown of the Stokes–Einstein relation near  $T_g$  predicts the deviation for small molecules.

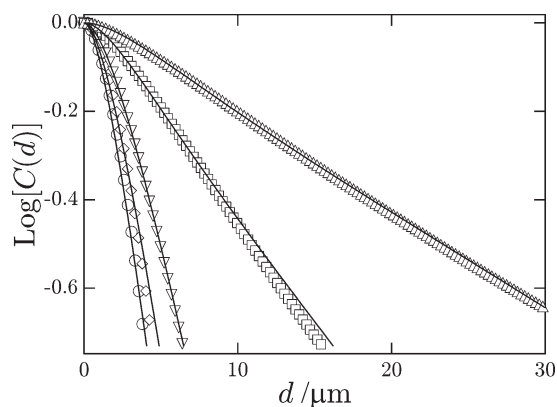
Figure 4 shows the POM images of the parts of itPS nonbanded spherulites, and Figure 5 shows the AFM images of lamellar crystals at the growth front of itPS spherulites. In those figures, it is clearly confirmed that the size of the patchy pattern in nonbanded spherulites and the width of lamellar crystals undergo consistent changes with crystallization temperature: the lower the temperature, the finer the structure, as expected from eq 1 or 2. Figure 6 shows the autocorrelation functions of eq 4 calculated for the spherulites at the respective temperatures in the plot against the distance along the radial direction,  $d$ . The plots could be well fitted by eq 5, indicating that the reorientation of lamellar crystals occurs in random directions to lose the correlation exponentially. The persistence length,  $L$ , of the correlation was determined by the fittings.

Figure 7 shows the persistence length,  $L$ , and the width of lamellar crystals,  $\lambda$ , plotted against crystallization temperatures. The proportional relationship between them can be seen in Figure 7, which confirms our previous conclusion with PE,<sup>1</sup> PVDF,<sup>2</sup> and itPB1<sup>3</sup> on the formation mechanism of the inner structure of spherulites determined by the width of the building blocks.

The data are also shown in the double-logarithmic plots against  $V\eta_T$  and against  $V\eta_T'$  in Figure 8. The slopes of the straight lines in Figure 8 are  $-0.60$  and  $-0.44$  for  $L$  and  $\lambda$ , respectively, when plotted against  $V\eta_T$ , while for the plots against  $V\eta_T'$ , the slopes are  $-1.9$  and  $-1.7$  for  $L$  and  $\lambda$ , respectively. Compared to the predicted slope of  $-0.5$  from eq 2, the slopes for the plots against  $V\eta_T$  are not far from the value, while those for  $V\eta_T'$  significantly deviated from the value. This result suggests the followings. First, the dependences of  $L$  and  $\lambda$  on  $V\eta_T$  well follows the predicted dependence of eq 1 or 2. Since the self-diffusion of long chain polymers is believed to couple with viscosity even at temperatures near  $T_g$  in the bulk melt, the distinction between the temperature dependence of self-diffusion and that of the inverse of viscosity is not possible with the present results.



**Figure 5.** AFM images (amplitude images) of the growth front of itPS spherulites crystallized at (a) 140, (b) 150, (c) 160, (d) 170, (e) 180, and (f) 190 °C. The image size is  $3.3 \mu\text{m} \times 3.3 \mu\text{m}$ .



**Figure 6.** Autocorrelation function,  $C(d)$ , determined from the images in Figure 4 of itPS spherulites crystallized at 150 (○), 160 (◇), 170 (▽), 180 (□), and 190 °C (△).

On the other hand, as expressed by  $\eta_T'$ , even though the diffusion of a portion of polymer chains on crystallizing may be specific at the growth front and can decouple from viscosity, the deviation of the slopes ( $-1.9$  and  $-1.7$ ) of  $L$  and  $\lambda$  from the predicted value of  $-0.5$  suggests that the diffusion of crystallizing portion of polymer chains at the growth front is not relevant to the structural formation of the lamellar width or of the spherulite. The results will be reasonable because the compositional

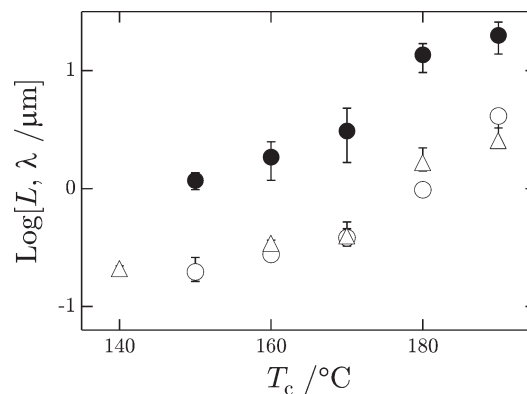


**Figure 7.** Semilogarithmic plots against crystallization temperature of the persistence length,  $L$  (●), determined from the decay of the autocorrelation function, such as shown in Figure 6, and the width,  $\lambda$  (○, in vacuum; △, in air), of lamellar crystals at the growth front observed by AFM.

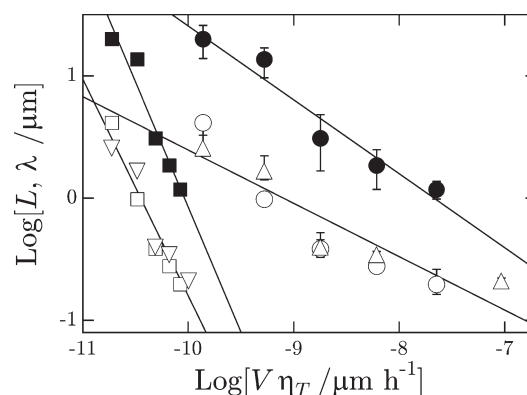


**Figure 8.** Double-logarithmic plots of  $L$  and  $\lambda$  in Figure 7:  $L$  (●) and  $\lambda$  (○, in vacuum; △, in air) against  $V\eta_T$  and  $L$  (■) and  $\lambda$  (□, in vacuum; ▽, in air) against  $V\eta_T'$ . The slopes of the fitting lines are  $-0.60$  (●),  $-0.44$  (○, △),  $-1.9$  (■), and  $-1.7$  (□, ▽), respectively.

gradient, which may be formed near the growth front, will be influenced by the self-diffusion of whole polymer chains in much wider length scale near the growth front. It means that the local diffusion affecting the growth rate is believed to be different from the global diffusion (in proportion to the inverse of viscosity), but the local diffusion does not affect the global structural evolution such as the branching instability supposed to be induced by the global compositional gradient or by pressure gradient. The successful fitting with  $(V\eta_T)^{-1/2}$  also excludes the possibility of the compositional gradient formed by small molecules as an impurity, with which the diffusion is expected to decouple from viscosity of polymer melt near  $T_g$ .

In the final part of discussion, it is worth mentioning about prior studies. After the general proposal<sup>6</sup> of the formation mechanism of spherulites based on the instability driven by a compositional gradient of uncrystallized molecules with the experimental support of OM images of branching itPS crystals grown from thin films,<sup>13</sup> Keith and Padden<sup>14</sup> and Basset and Vaughan<sup>15</sup> have attempted to examine the correlation predicted by the modeling. They have examined itPS spherulites but did not find the expected correlation between the diffusion length,  $D/V$ , and the length scale of lamellar structures, which can be the lateral width or the size of lamellar fibrils. We think that the unsuccessful observations of the relationship were partly due to the prediction of the proportional relationship between them, which must be much weaker square root dependence expressed as eq 1 with the contribution of stabilizing effect of surface tension.<sup>21</sup> In addition, the temperature range examined was higher than



200 °C, where the morphology of itPS spherulite is much coarser than that examined in our experiments in the range mainly below 200 °C. In the high temperature range, the inner structure is too coarse to be characterized by the patchy pattern and only shows a weak variation in the pattern. As we have suggested, the inner structure and the width of lamellar crystals are in proportion to each other. The crystallization condition needs to be wide enough to have large variations of the inner structure as well as of the lamellar width. For the high temperature range they examined, we suppose that the effect of the gradient field gets weaker and difficult to be confirmed. In the temperature range we examined, the persistence length of the inner structure changed with temperature by more than 1 order in magnitude, so that we could also expect the change in the lateral width of lamellar crystals in the same order.

Concerned with the reorientation of lamellar crystals in polymer spherulites, historically, we are also aware of the explanations for the lamellar twisting in banded spherulites, based on the elastic lamellar twist due to unbalanced surface stresses<sup>22,23</sup> and on the sequential creation of axial screw dislocations of the same handedness with thermal activation.<sup>24</sup> In the modeling, the inner structure of banded spherulites, namely the band spacing, is determined not by the lamellar width but by the lamellar thickness. The modeling predicts that thinner lamellae are more susceptible to twist because the unbalanced surface stresses caused by chain folds are localized on the folding surfaces. The modeling of elastic twist predicts a parabolic dependence on lamellar thickness,  $\ell$ , of the band spacing,  $P$ :  $P \propto \ell^2$  with the coefficient determined by the elastic modulus, excess surface tension, and the thickness of the surface regions. On the other hand, since the creation of axial screw dislocation needs the elastic energy in proportion to  $\ell^3$ , the thermal activation process predicts an exponential dependence on the lamellar thickness of the band spacing:<sup>24</sup>  $P \propto \exp[C_{\text{dis}}\ell^3/k_B T]$  with the coefficient,  $C_{\text{dis}}$ , derived from the elastic modulus of crystals for the creation of screw dislocation. In our previous paper<sup>1</sup> on the formation of banded spherulites of polyethylene, we have quantitatively examined the predictions of the modeling. First, the modeling of the elastic twist was dismissed because the dependence of  $P$  on  $\ell$  showed much stronger dependence with the power of 9.2. For the second modeling of thermal activation of defects formation, the obtained coefficient,  $C_{\text{exp}} \approx 8 \times 10^3 \text{ J/m}^3$ , was much smaller than the calculated value ( $C_{\text{dis}} \geq 10^8 \text{ J/m}^3$ ) by orders of magnitude. This result suggested almost perfect compensation of the strain energy of dislocation by that of surface strain, which is quite unlikely.

For the nonbanded spherulites of itPS, similar examination can be made for the persistence length of the patchy pattern,  $L$ , because the surface stresses are believed to be the origin of the loss of correlation of lamellar orientation by twisting in random directions. Then, it is possible that the persistence length is determined by the susceptibility of lamellar crystals to the elastic twist or to the creation of screw dislocations, which are dependent on the lamellar thickness in the same manner as those for banded spherulites. Figure 9 shows the persistence length plotted against the crystalline lamellar thickness,  $\ell$ , determined by Fukao and Miyamoto<sup>26</sup> for the same material. As shown in Figure 9a, the dependence of  $L$  on  $\ell$  is much stronger than the predicted parabolic law and fitted with the power of 8.6. On the other hand, the coefficient of the fitting in the semilogarithmic plot of Figure 9b is  $C_{\text{exp}} \approx 1.2 \times 10^6 \text{ J/m}^3$  and much smaller than the calculated value for PE crystals. Though the shear modulus of itPS crystals is not available, unlike with the Young's modulus directly depending on the backbone structure, the shear modulus of polymer crystals seems to be weakly dependent on polymer species. Therefore, the coefficient for itPS will not be different in orders of magnitude. In this way, we come to the same conclusion

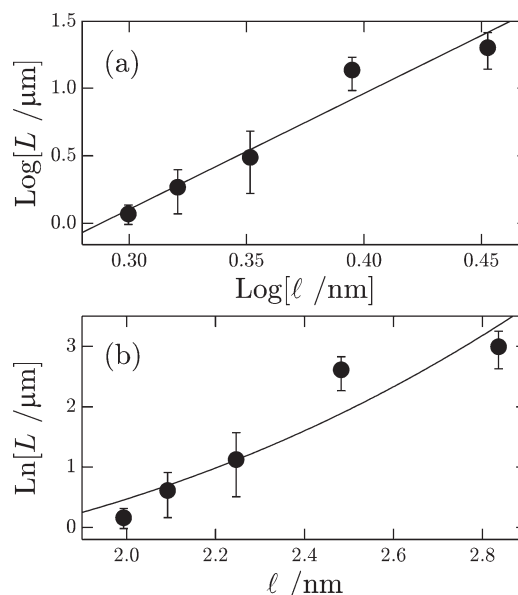


**Figure 9.** Plots of the persistence length,  $L$ , against crystalline lamellar thickness,  $\ell$ , determined by Fukao and Miyamoto:<sup>26</sup> (a) double-logarithmic and (b) semilogarithmic plots. The fitting line in (a) represents  $L \propto \ell^{8.6}$  and in (b)  $L \propto \exp[C_{\text{exp}}\ell^3/k_B T]$  with  $C_{\text{exp}} = 1.2 \times 10^6 \text{ J/m}^3$ .

on the unsuccessful approaches by the explanations solely based on the effects of lamellar thickness. It is noted that those results do not dismiss either of the cases of continuous reorientation along the lamellar crystals or the discontinuous reorientation with the formation of screw dislocation. In terms of the formation of screw dislocation, our modeling suggests that the formation is not the cause of the branching but the consequence of branching due to instability. Actually, recent observations by in situ SPM of polymer crystallization suggest unstable growth front of individual crystals, which eventually evolve branching to form spiral terraces as the consequence.<sup>27,28</sup>

Finally, we discuss the approach by Granasy et al.<sup>29</sup> on the formation mechanism of spherulites. Spherulites are formed not only by polymers. The formation is a general feature of crystallization when crystallized from e.g. viscous media. Therefore, the formation mechanism is a quite important issue to be clarified not only for polymer physics but for the understanding of crystal growth in general and for the practical applications. Granasy et al.<sup>29</sup> have suggested a modeling based on the dynamic heterogeneities caused by the decoupling of translational diffusion from orientational relaxation near  $T_g$ . They supposed the heterogeneities as the source of grain nucleation at the growth front for the formation of branches to fill in the structure. Concerned with polymers, the decoupling near  $T_g$  has been experimentally dismissed.<sup>12</sup> The possibility of decoupling may still be supposed for the crystallizing portion of polymer chain at the growth front if the mobility of the portion is different from that in the bulk melt. However, it is also known that spherulites of a number of polymers are formed at temperatures much higher than  $1.2T_g$ , while the decoupling extends only below this temperature. For polymer spherulites, they have supposed that a fixed angle of misorientation of splaying plays a crucial role for the formation of branches.<sup>30</sup> We think that the reorientation on branching in our modeling will be the source of this type of misorientation.

#### 4. Conclusion

We have experimentally examined the kinetics and morphology on the crystallization of itPS spherulites near  $T_g$ , at which the spatial heterogeneity is believed to develop in the melt with lowering the temperature. The heterogeneity introduces

the decoupling of diffusion of small molecules in the melt from polymer melt viscosity and hence possibly influences the kinetics and morphology for the growth of itPS spherulites. In terms of the kinetics of crystallization, we have reconfirmed the deviation of the growth rate data from the adjustment by the mobility factor represented by the melt viscosity. The deviation has been assigned to the characteristic feature for the mobility of crystallizing portion of polymer chain. We have suggested that the deviation may be caused by the decoupling from melt viscosity for the diffusion of crystallizing portion just at the growth front near  $T_g$ .

In terms of the morphology, the inner structure of the non-banded itPS spherulites was characterized by the persistence length of the patchy pattern observed by POM. The lamellar crystals at the growth front of spherulites were observed by AFM for the films isothermally crystallized, quenched to stop the growth, and chemically etched subsequently. As has been confirmed for the banded spherulites of PE<sup>1</sup> and PVDF<sup>2</sup> and the nonbanded spherulites of itPBI,<sup>3</sup> we have reconfirmed the proportional relation between the characteristic length of the inner structure of spherulites and the width of the building blocks, which is the width of lamellar crystals at the growth front.

In terms of the correlation between the morphological characteristics and the kinetics of crystallization, based on our proposal of the instability-driven branching for the formation of polymer spherulites, we have examined the temperature dependences of the persistence length and the width of growth front in the logarithmic plots against the crystal growth rate multiplied by the temperature dependence of viscosity. The results confirmed the expected dependence scaled with the melt viscosity, as for PE,<sup>1</sup> PVDF,<sup>2</sup> and itPBI.<sup>3</sup> In our modeling, the instability is caused by a self-organized gradient field ahead of the growth front. We have suggested two possible gradient fields, such as the compositional gradient formed by uncrystallized molecules excluded from the growth front and the pressure gradient required for the stationary growth, to compensate for the density difference between the crystal and the melt. Owing to the coupling of self-diffusion of whole polymer chain with the melt viscosity even at the temperatures near  $T_g$ , the present results well explained by the temperature dependence of melt viscosity do not differentiate the compositional gradient determined by the self-diffusion of whole chain and the pressure gradient by melt viscosity. The results dismiss the influence of the decoupled self-diffusion of crystallizing portion of polymer chain on the morphological evolution by the instability. The possible influence of the compositional gradient formed by small molecules behaving as an impurity is also excluded.

**Acknowledgment.** The authors thank Prof. S. Tanaka of Hiroshima University, Prof. Y. Yamazaki of Waseda University,

Prof. T. Taniguchi of Kyoto University, and Prof. H. Tanaka of University of Tokyo for helpful discussions. This work was supported by KAKENHI (Grant-in-Aid for Scientific Research) on Priority Area "Soft Matter Physics" from the Ministry of Education, Culture, Sports, Science and Technology of Japan.

## References and Notes

- (1) Toda, A.; Okamura, M.; Taguchi, K.; Hikosaka, M.; Kajioaka, H. *Macromolecules* **2008**, *41*, 2484.
- (2) Toda, A.; Taguchi, K.; Hikosaka, M.; Kajioaka, H. *Polym. J.* **2008**, *40*, 905.
- (3) Kajioaka, H.; Hikosaka, M.; Taguchi, K.; Toda, A. *Polymer* **2008**, *49*, 1685.
- (4) Toda, A.; Taguchi, K.; Kajioaka, H. *Macromolecules* **2008**, *41*, 7505.
- (5) Lotz, B.; Cheng, S. Z. D. *Polymer* **2005**, *46*, 577.
- (6) Keith, H. D.; Padden, F. J., Jr. *J. Appl. Phys.* **1963**, *34*, 2409.
- (7) Schultz, J. M. *Polymer Crystallization*; Oxford University Press: Oxford, 2001; Chapter 10.
- (8) Pearson, D. S.; Ver Strate, G.; von Meerwall, E.; Schilling, F. C. *Macromolecules* **1987**, *20*, 1133.
- (9) Hoffman, J. D.; Davis, G. T.; Lauritzen, J. I., Jr. *Treatise on Solid State Chemistry*; Plenum Press: New York; 1976; Vol. 3, Chapter 7.
- (10) Richert, R. *J. Phys.: Condens. Matter* **2002**, *14*, R703.
- (11) Wang, C.-Y.; Ediger, M. D. *Macromolecules* **1997**, *30*, 4770.
- (12) Urakawa, O.; Swallen, S. F.; Ediger, M. D.; von Meerwall, E. D. *Macromolecules* **2004**, *37*, 1558.
- (13) Keith, H. D. *J. Polym. Sci.* **1964**, *A2*, 4339.
- (14) Keith, H. D.; Padden, F. J., Jr. *J. Polym. Sci.* **1987**, *B25*, 2371.
- (15) Bassett, D. C.; Vaughan, A. S. *Polymer* **1985**, *26*, 717.
- (16) Vaughan, A. S.; Bassett, D. C. *Polymer* **1988**, *29*, 1397.
- (17) Kajioaka, H.; Taguchi, K.; Toda, A., manuscript in preparation.
- (18) Ferry, J. D. *Viscoelastic Properties of Polymers*, 3rd ed.; Wiley: New York, 1980.
- (19) Kim, S. H.; Teymour, F.; Debling, J. A. *J. Appl. Polym. Sci.* **2007**, *103*, 2597.
- (20) Lovinger, A. J.; Davis, D. D.; Padden, F. J., Jr. *Polymer* **1985**, *26*, 1595.
- (21) Mullins, W. W.; Sekerka, R. F. *J. Appl. Phys.* **1963**, *34*, 323; 1964, *35*, 444.
- (22) Hoffman, J. D.; Lauritzen, J. I., Jr. *J. Res. Natl. Bur. Stand.* **1961**, *65A*, 297.
- (23) Okano, K. *Jpn. J. Appl. Phys.* **1964**, *3*, 351.
- (24) Schultz, J. M.; Kinloch, D. R. *Polymer* **1969**, *10*, 271.
- (25) Shadrake, L. G.; Guieu, F. *Philos. Mag.* **1976**, *34*, 565.
- (26) Fukao, K.; Miyamoto, Y. *Polymer* **1993**, *34*, 238.
- (27) Hobbs, J. K.; Humphris, A. D. L.; Miles, M. J. *Macromolecules* **2001**, *34*, 5508.
- (28) Xu, J.; Guo, B.-H.; Zhang, Z.-M.; Zhou, J.-J.; Jiang, Y.; Yan, S.; Li, L.; Wu, Q.; Chen, G.-Q.; Schultz, J. M. *Macromolecules* **2004**, *37*, 4118.
- (29) Gránásky, L.; Pusztai, T.; Börzsönyi, T.; Warren, J. A.; Douglas, J. F. *Nat. Mater.* **2004**, *3*, 645.
- (30) Gránásky, L.; Pusztai, T.; Tegze, G.; Warren, J. A.; Douglas, J. F. *Phys. Rev. E* **2005**, *72*, 011605.